ACS APPLIED MATERIALS & INTERFACES

Research Article

www.acsami.org

Molecularly Engineered Azobenzene Derivatives for High Energy Density Solid-State Solar Thermal Fuels

Eugene N. Cho, David Zhitomirsky, Grace G. D. Han, Yun Liu, and Jeffrey C. Grossman*

Department of Materials Science and Engineering, Massachusetts Institute of Technology, Cambridge, Massachusetts 02139, United States

Supporting Information

ABSTRACT: Solar thermal fuels (STFs) harvest and store solar energy in a closed cycle system through conformational change of molecules and can release the energy in the form of heat on demand. With the aim of developing tunable and optimized STFs for solid-state applications, we designed three azobenzene derivatives functionalized with bulky aromatic groups (phenyl, biphenyl, and *tert*-butyl phenyl groups). In contrast to pristine azobenzene, which crystallizes and makes nonuniform films, the bulky azobenzene derivatives formed uniform amorphous films that can be charged and discharged with light and heat for many cycles. Thermal stability of the films, a critical metric for thermally triggerable STFs, was greatly increased by the bulky functionalization (up to 180 °C), and we were able to achieve record high energy density of 135 J/g for solid-state STFs, over a 30% improvement compared to previous solid-state reports. Furthermore, the chargeability in the solid state was improved, up to 80% charged from 40% charged in previous solid-state reports. Our results point toward molecular engineering as an effective method to increase energy storage in STFs, improve chargeability, and improve the thermal stability of the thin film.

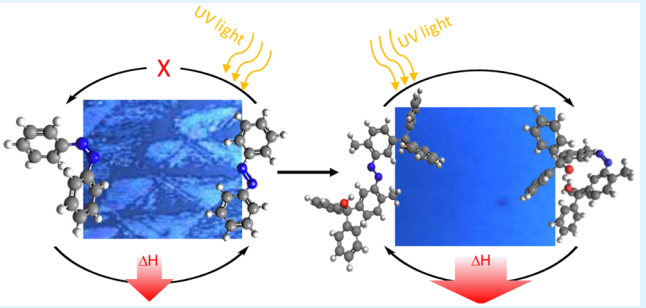

KEYWORDS: *solar thermal fuels heat storage, molecular thin films, solid-state applications, structural design, molecular engineering, photoswitching*

INTRODUCTION

Despite the vast abundance of solar radiation, efficient conversion, storage, and distribution of this resource remains a challenge. One approach that uses the same material to both convert and store the sun's energy is the use of photoactive molecules. These molecules convert solar energy into strained or rearranged chemical bonds, with the amount of energy stored, ΔH, as the difference in energy between the ground and metastable states. Upon reversion back to the ground state, the energy is released in the form of heat with the molecules back in their ground state ready to be charged again. These materials for solar energy harvesting, referred to as solar thermal fuels (STF), operate in a closed cycle and ideally possess high energy density and cyclability with no degradation or emissions and easy distribution as "heat on demand".

Previous work on candidate solar thermal fuels has shown both promise and many challenges in optimizing the required properties. For example, norbornadiene showed great potential with high energy density (89 kJ/mol). Although cyclability has been the biggest challenge, recent research by molecular modification of norbornedine using aryl substituents showed improvement of cyclability.[1−3] Recent work showed that (Fulvalene) tetracarbonyl-diruthenium showed reasonable gravimetric energy density (30.6 Wh/kg) while showing high cyclability, but due to the use of expensive ruthenium, its potential is limited.[4,5] Azobenzene possesses high cyclability but has been hindered by low energy density.[6] Recently, several templating methods of the solar thermal fuel molecule have gained attention and have been investigated for solid-state STF applications.[7−12] Some of the templates include carbon nanotubes, polymers, and diacetylene.

Of these, the polymer approach has thus far proved most successful, allowing robust solid-state STF[10] and controlled thickness.[13] Solid-state STF opens a window to a range of applications by integrating STF materials to existing solid-state devices such as coatings for deicing, solar blankets and functional fibers, or implementation in new novel solid state energy devices for consumer oriented heating equipment. However, templating the solar thermal fuel molecule onto a polymer presents limitations in chargeability in the solid state and shows a substantial reduction in energy storage compared to the monomer.

Here, we overcome these limitations by revisiting the design of purely molecular azobenzene-based derivatives targeted for solid-state solar thermal fuels. Previous work showed that pristine azobenzene results in poor film morphology due to

Received: November 22, 2016
Accepted: February 24, 2017
Published: February 24, 2017

DOI: 10.1021/acsami.6b15018
ACS Appl. Mater. Interfaces XXXX, XXX, XXX−XXX

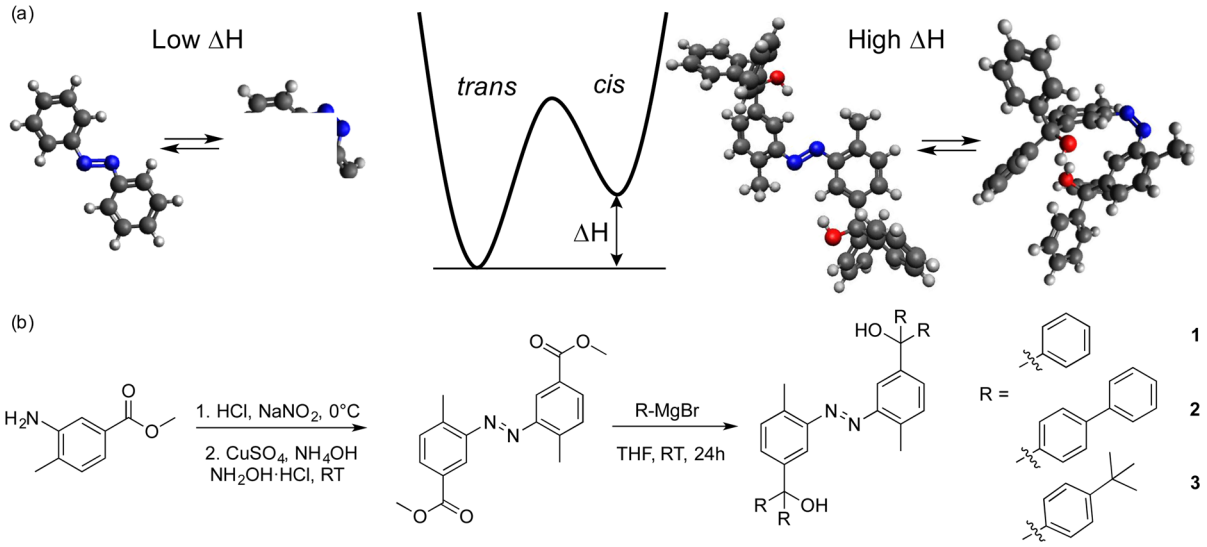

Figure 1. (a) Comparison of *trans* and *cis* forms of pristine azobenzene and the *trans* and *cis* forms of functionalized azobenzene predicted computationally (referred to as compound **1**).[27] The energy diagram and the difference in energy stored ΔH is shown. (b) Schematic of synthesis of compounds **1**−**3** via the diazotization of an aniline precursor followed by the addition of different aryl groups using Grignard reagents.

crystallization, which prevents photoisomerization of the molecule.[14] Solid-state forms of azobenzene have been achieved via functionalization onto gold surfaces,[15,16] polymer backbones,[17−19] Langmuir−Blodgett films,[20−22] and in the form of liquid crystals.[23−25] Here, we opt for a molecular design of solid-state azobenzene films toward the goal of high efficiency STF applications, where film morphology must be optimized concomitant with energy density, cyclability, and thermal stability. Past efforts to modify azobenzene to increase its energy density, e.g., by adding substituents, have resulted in the deterioration of other favorable traits such as the thermal reversion lifetime or absorption spectrum.[26] Past computational work on solar thermal fuels revealed that decorating photoswitches with functional groups could result in property enhancement due to both intermolecular[7] and intramolecular[27] interactions. With the aim of probing these sometimes competing properties and using computational work as guidance, here we synthesize and characterize three molecules based on tailored modification of azobenzene. In this work, we choose functional groups that could promote improved solar thermal properties while simultaneously resulting in switchable amorphous thin films. Suitable chemical modification of azobenzene would ideally maintain photoswitchability while increasing the energy stored per molecule, improve thermal robustness, and stabilize a uniform film morphology in both the charged and ground states.

EXPERIMENTAL DETAILS

UV−Vis Measurement. Solution state absorption was carried out using a Cary60 equipped with a Quantum Northwest TLF 50 temperature controller. Thirty-nine micromolar concentration of compound **1** and azobenzene in chloroform were measured in a 10 mm path length quartz cuvette at 25 °C. Solid-state UV−vis measurements were performed using a Cary5000 instrument on a 1in quartz disks. Charging was done by 365 nm wavelength 100 W lamp, while discharging was done by heat at 100 °C or visible light in air.

HPLC Measurement. Agilent 1290 UPLC system equipped with a 6150 single quadrupole mass spectrometer was used for the measurement separated using column (Zorbax Eclipse Plus C18 Rapid Resolution HD 2.1 × 50 mm column with 1.8 μm particles) maintained at 25 °C. Single direct injections were introduced via a bypass loop in a Syrris AFRICA Sampler and Diluter, which diluted samples by a factor of 5−10 before transferring them into the high-pressure flow path of the UPLC.

Image Acquisition. Images of the thin films were obtained using a conventional optical microscope. High magnification images of the thin films were obtained using Zeiss Merlin scanning electron microscope (SEM) on a single crystal silicon substrate.

Differential Scanning Calorimetry (DSC) Measurements. Samples were charged in a stirring solution using 365 nm 100W UV lamp while being cooled at 20 °C until a photostationary state was achieved. The solution was then concentrated by drying the solvent, which was transferred to the DSC pan and then fully dried under vacuum. The measurement was taken at a rate of 5 °C/min. The ratio between the *cis* and *trans* was obtained using HPLC. The measurement was taken using TA Instruments DSC Q20.

Solid-State Sample Preparation. The solid-state STF samples were prepared in THF-based solution of azobenzene and compound **1** with 30 and 25 mg/mL, respectively. The THF-based solution was then dropcasted onto a 1 in quartz disk and spin-coated at 1000 rpm. Compound **2** and compound **3** solid-state samples were produced similarly using 45 and 50 mg/mL solutions of THF, respectively. The film thickness of the sample varied between 400 and 600 nm.

Raman Spectroscopy and Fluorescence Spectra. Raman spectroscopy and fluorescence spectra were done on a Horiba Labram HR800 Raman spectrometer using a He−Ne laser (633 nm wavelength) through a 100× objective. The solid-state samples were dropcasted from chloroform for all three of the compounds. The measurements were done on a temperature control module. The temperature resolved fluorescence spectra were taken on the *cis* state film of compound **1**, the temperature being ramped up at 5 °C/min. The *trans* state film was done similarly but stopped every 25 °C and held for 5 min for compound **1**, compound **2**, and compound **3**. Optical images of the film were taken during each stop.

X-ray Diffraction (XRD). XRD was done on Bruker D8 Discover GADDS with a stationary area detector with the center at 30° (2θ). The sample to detector distance was 16.25 cm. The sample was prepared by dropcasting methods with solution of compound **1**, **2**, and **3** in THF with concentrations of 20, 40, and 46 mg/mL. The solution was dropcasted onto 100 orientation silicon substrate with the substrate heated to 45 °C. The variation of temperature was done ex situ by heating the sample on a hot plate for 5 min at temperatures starting at 25 °C with increments of 25 °C up to 150 °C. XRD measurements were taken at each step.

DOI: 10.1021/acsami.6b15018
ACS Appl. Mater. Interfaces XXXX, XXX, XXX−XXX

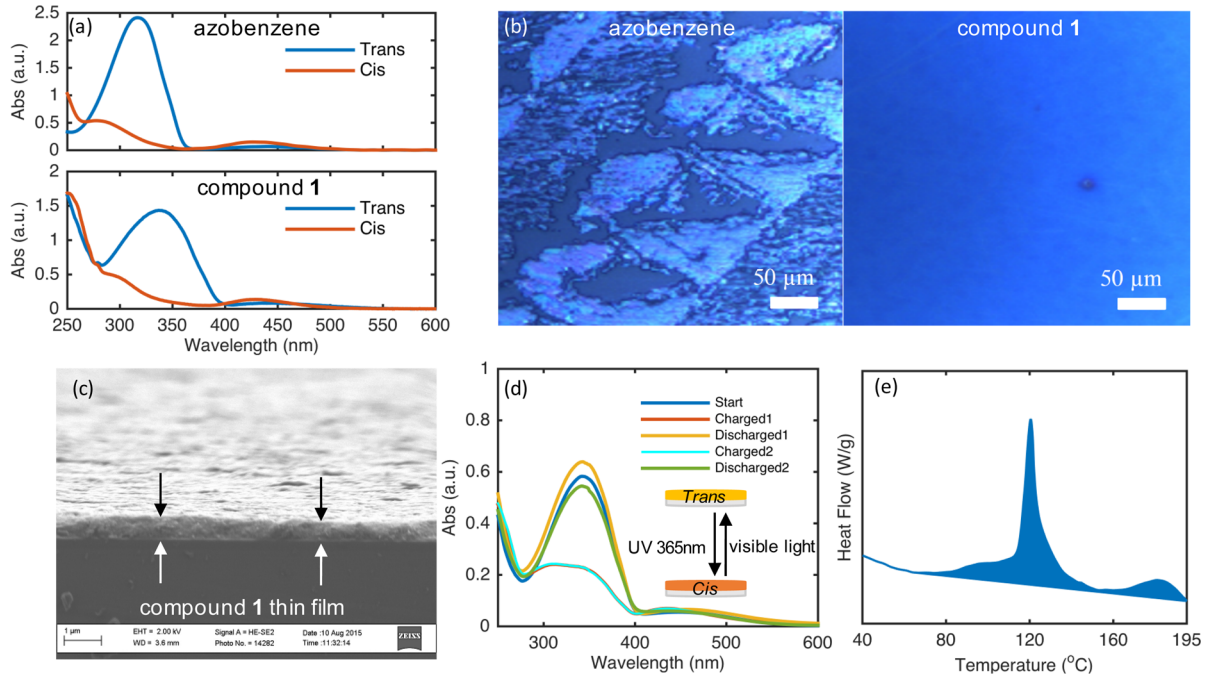

Figure 2. (a) UV−vis absorption spectra of azobenzene (top) and compound **1** (bottom) for comparison, showing a red shift in the *trans* $\pi \rightarrow \pi^*$ transition from azobenzene to compound **1**. (b) Optical image of spin coated azobenzene (left) and compound **1** (right) on quartz disks. (c) Cross-sectional SEM of compound **1** film. (d) UV−vis spectra of compound **1** film upon cycling via UV and visible light. The red line (charged 1) is behind the cyan line (charged 2). (e) DSC trace of 95% *cis* compound **1** at 5 °C/min scan rate.

Solid-State Chargeability Measurements. The chargeability measurement was done by charging the sample ex situ with UV light and characterized with solid-state UV−vis measurements. Samples of compounds **1**, **2**, and **3** were prepared by spin-coating on a 1 in. quartz disc with the solution concentration of 0.06 M in THF for each compound. The sample was then heated to 50 °C for 2 h to remove any residual solvent while allowing the film to change to the *trans* state. The sample was exposed to the 365 nm light for 20 s at a time in the beginning. After each exposure, solid-state UV−vis measurements were taken. As the change in the absorption decreased, the exposure time was gradually increased up to 60 s.

RESULTS AND DISCUSSION

Design of Solid-State STF Molecules. When *trans* azobenzene (Figure 1a) is exposed to UV light (300−365 nm), the molecule photoisomerizes to the higher energy *cis* state. A modified molecule was selected base on criteria from computational work[7,27] that is expected to increase the *cis*/*trans* energy difference, shown on the right side of Figure 1a (referred to henceforth as compound **1**). The addition of a bulky phenyl group causes the *cis* form to achieve a higher energy state due to the repulsion and steric hindrance, increasing the energy difference (ΔH) between the *trans* and *cis* states. Beyond increased energy density, the addition of bulky phenyl groups to the azobenzene base molecule is expected to improve solid-state film formation by promoting amorphous thin films, although the interplay between energy density, photoswitchability, crystallization, and temperature robustness is unknown. To understand and explore these properties further, we synthesized two additional variations, one with the addition of a biphenyl group (compound **2**) and one with a *tert*-butyl phenyl group (compound **3**). The synthesis of these three molecules is shown schematically in Figure 1b where, starting from the precursor material, a two-step process was adapted from previous work on the synthesis of compound **1** for catalyst applications.[28]

Optical and Thermal Properties of Compound 1. The azobenzene molecule possesses two main absorption features resulting from the $\pi \rightarrow \pi^*$ and n $\rightarrow \pi^*$ transitions (Figure 2a, top). In the *trans* state, the dominant $\pi \rightarrow \pi^*$ transition absorption peak lies at 325 nm, and the much weaker n $\rightarrow \pi^*$ absorption peak is at 450 nm. When the molecule is photoisomerized to the *cis* state, the $\pi \rightarrow \pi^*$ transition peak disappears, while the n $\rightarrow \pi^*$ peak shifts to 430 nm. For compound **1**, the $\pi \rightarrow \pi^*$ transition red shifts to 347 nm in the *trans* state with little change for the n $\rightarrow \pi^*$ absorption upon photoexcitation to the cis state (Figure 2a, bottom). Exposure to a 365 nm wavelength UV light source at the photostationary state (over 12 h exposure) gives a *trans*:*cis* ratio of 5:95, as confirmed by liquid chromatography−mass spectrometry (LC−MS). Comparison of spin-coated thin-films under optical microscope reveals nonuniform morphology for the pristine azobenzene material (Figure 2b, left) and smooth crack-free coverage for compound **1** (Figure 2b, right). A cross-sectional SEM image (Figure 2c) of compound **1** confirmed the uniform thickness of the film. The difference in film morphology between azobenzene and compound **1** is due to the bulky phenyl groups on the tertiary carbon center on the *meta* position of the azobenzene molecule in compound **1**, which causes a break in the planarity of the structure, preventing the molecules from crystallizing.[29,30] This allows photoisomerization of solid-state thin films of compound **1**. Retention of absorption characteristics was verified by comparing solution and solid-state spectra, which indicated minimal change in the spectra (Supporting Information, S5). Optical cycling experiments in solution and NMR of compound **1** in solution after extended period in room light can be seen in the Supporting Information, S6 and S7. Photoinduced isomerization was used

DOI: 10.1021/acsami.6b15018
ACS Appl. Mater. Interfaces XXXX, XXX, XXX−XXX

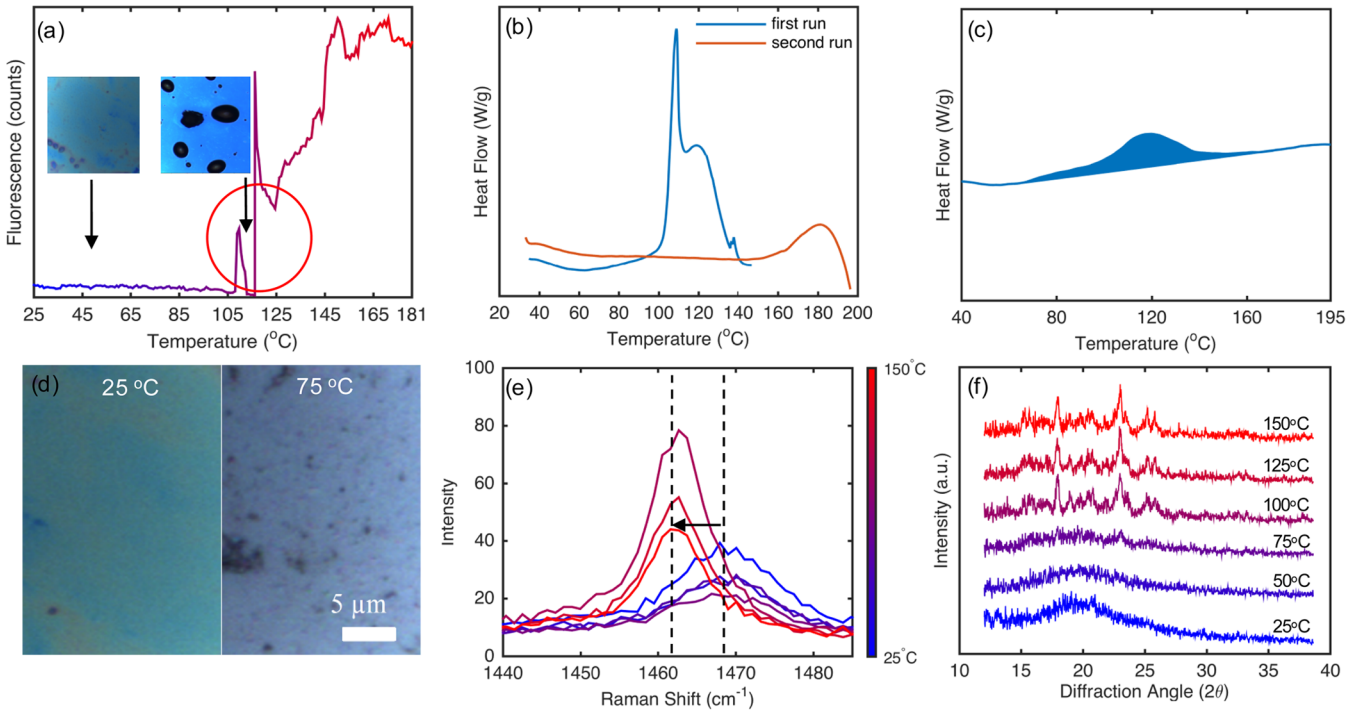

Figure 3. (a) Temperature resolved fluorescence spectra of *cis* compound **1** in the film state. Temperature vs fluorescence spectra was averaged over a range from 1250 to 1350 cm^{-1}. The temperature of the stage was ramped at a rate of 5 °C/min. The drop in the signal is due to the film undergoing morphological change into a droplet and the laser losing the target. At around 107 °C, the fluorescence count increases as compound **1** aggregates and forms droplets. This phenomenon is seen in only *cis* compound **1** dominant films and not in *trans* compound **1** dominant films. (b) DSC of 82% *cis* compound **1** sample. The sample was ramped to 150 °C the first run (blue) and then to 200 °C in the second run (orange). (c) DSC of 35% *cis* compound **1** sample. (d) Left: optical image of *trans* dominant compound **1** film on silicon at 25 °C. Right: optical image of *trans* dominant compound **1** molecular film on silicon at 75 °C. (e) Temperature resolved Raman mapping of *trans* compound **1** in the film state. The temperature of the stage was ramped at a rate of 5 °C/min. The shift from 1469 to 1462 cm^{-1} and the increase in the sharpness of the peak indicates that the molecular thin film system is in a more crystalline state. (f) Ex situ temperature XRD on compound **1** film (scan time 60 s).

to test the charging and discharging properties of the films with UV light at 365 nm at room temperature to charge the film (12 h) and visible light (3 h) to discharge the film. The state of the film was measured using UV−vis absorption with two cycles taken for compound **1**, as shown in Figure 2d, and no visible morphology change was observed over such optical cycles. This switchability in the solid-state for the compound **1** film is in contrast to that of azobenzene, for which the crystal structure prevents isomerization under illumination due to the lack of free volume.[31]

The enthalpy difference between *cis* and *trans* isomers was determined using DSC in the solid-state (Figure 2e), which showed a heat release (4 measurements) of 134 ± 6 J/g or 77 ± 3 kJ/mol for compound **1**, significantly larger than that of azobenzene (~49 kJ/mol) and over a 30% increase from the polymer azobenzene.[6,10] In contrast to azobenzene and azobenzene template structures that typically yield one exothermic peak for the *cis* to *trans* release of stored heat,[9,10,32,33] compound **1** showed two peaks, which reveals an important aspect of processing small-molecule films as STF materials, as will be discussed below.

Analysis of Thermal Properties of Compound 1. Thermal isomerization properties can change depending on the environment in which the azobenzene molecule is placed.[34,35] To further understand the DSC results, the morphology change of the compound **1** film under varying temperatures was analyzed using an optical microscope and Raman spectroscopy. A *cis* compound **1** film was made by dropcasting a solution of compound **1** in chloroform that has reached the photostationary state (~95% *cis*) through illumination. The dropcasted film showed relatively uniform morphology. At around 107 °C, the *cis* compound **1** molecular film was observed under the optical microscope to form the droplets (Figure 3a) as well as a drastic increase in fluorescence. The sudden drop in the fluorescence to zero at 107 °C is due to the formation of the droplet and the laser losing the compound **1** target. The laser was immediately refocused on the droplet for the measurement shown by the recovery of the fluorescence signal. Increased fluorescence occurs in azobenzene when the conformational freedom is restricted and isomerization is inhibited by the surrounding environment.[36,37] Fluorescence starts to decrease once enough thermal energy is present for the switching.[9] After peaking at 117 °C, the fluorescence decreased and then started to increase again at 125 °C, showing that the conformational freedom is restricted once more.

To test the effects of morphological changes, DSC was carried out on an 82% cis sample, ramped once to 150 °C, cooled to 25 °C, then ramped to 200 °C (Figure 3b). This showed a single peak during each of the ramps, indicating that the two peaks arise from separate populations of molecules. Steric hindrance and local environment affects the thermal isomerization process, affecting the thermal isomerization kinetics.[34,35] Thus, the cause of the two peaks is related to the inherent morphological changes experienced by the *cis* film as temperature increases, resulting in different subpopulations of azobenzene that release heat at different rates due to their local steric environments.

DOI: 10.1021/acsami.6b15018
ACS Appl. Mater. Interfaces XXXX, XXX, XXX−XXX

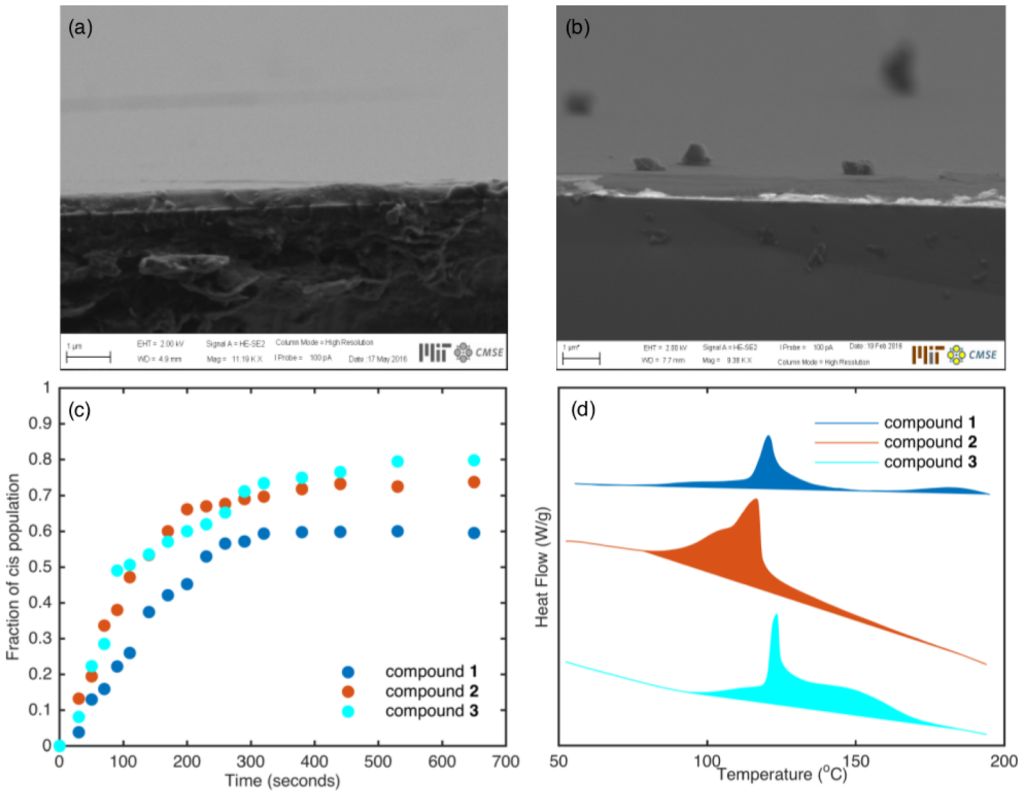

Figure 4. (a) Cross-sectional SEM of the compound **2** film. (b) Cross-sectional SEM of the compound **3** film. (c) Chargeability of compounds **1**, **2**, and **3**. The process was done ex situ, where the sample was charged under 365 nm UV light for a set time, and then solid-state UV−vis spectra was taken. (d) DSC traces for compounds **1**, **2**, and **3** from top to bottom. The *y*-direction represents heat release, and the region enclosed with the flat baseline represents the area integrated to obtain energy release.

DSC for samples (5 measurements) of a *trans* dominant film with ∼35% *cis* (Figure 3c) showed a single peak heat release. Considering the percentage of charged (*cis*) molecules and calculating the energy stored per molecule, this translates to $\Delta H = 81 \pm 3$ kJ/mol, which is similar to that of the 95% *cis* sample with two release peaks. No droplet formation was observed in a *trans* dominant compound **1** molecular film. A pristine film appears clear but after heating turns opaque at 75 °C (Figure 3d). To understand the thermal properties of the *trans* dominant film, temperature resolved Raman mapping was performed (Figure 3e). The peak between 1450 and 1500 cm^{-1} was measured as its position and shape are associated with the stretching of the N═N azo bond.[38−41] At 25 °C, the Raman peak is broad and centered at 1469 cm^{-1}, while at 75 °C, the peak shifts to 1462 cm^{-1} with a narrower width, signifying that the material has become more crystalline. This was further confirmed using ex situ temperature-dependent XRD shown in Figure 3f. The film at 25 °C showed a single broad XRD peak, which suggests that the film was in an amorphous state. When heated to 75 °C, sharp XRD peaks started to appear that translate to the formation of crystalline regions.

Compared to azobenzene, the added bulky phenyl to the carbon on the metaposition of azobenzene in compound **1** proved to be effective in improving the azobenzene molecule for purely molecular solid-state solar thermal fuel in three ways: (1) by red shifting the $\pi \rightarrow \pi^*$ transition absorption peak, allowing 95% charging of the material under 365 nm light source; (2) by preventing crystallization of the molecule at ambient conditions, allowing solid-state switching of the film; and (3) by increasing the energy stored per molecule. The increase in percent charged and increase in energy stored per molecule is important because, although the molecular weight of compound **1** is 3 times that of azobenzene, the gravimetric energy density is measured to be ∼134 J/g (37 Wh/kg), which is comparable to that of the azobenzene molecule and higher than that of the polymer template azobenzene by 30%.[10,26] The prevention of crystallization of compound **1** allows for the fabrication of stable, amorphous thin films. Crystallization (as in the case of pure azobenzene) presents a challenge for solid-state applications because the steric hindrance between the molecules in the crystal prevents the molecule from switching between the *trans* and the *cis* state. The fact that compound **1** films remain amorphous leads to much improved chargeability in the solid-state. This allows the individual molecule in the amorphous film to have the necessary free volume to achieve photoisomerization. However, the molecular film was not able to retain its original amorphous state when heated. When thermally triggered, the film needs to be able to withstand temperatures up to the reversion temperature. The *trans* rich film crystallized at around 75 °C while the *cis* rich film formed droplets at 105 °C. In both cases, the change in film morphology brought on by crystallization prevented the compound **1** film to charge from *trans* to *cis* after this thermally induced transformation. This crystallization hinders optical charging of the film because the crystal structure prevents isomerization through illumination due to the lack of free volume.[31] Thus, another strategy was needed for the film to retain its original amorphous state while allowing thermal switching of the material.

DOI: 10.1021/acsami.6b15018
ACS Appl. Mater. Interfaces XXXX, XXX, XXX−XXX

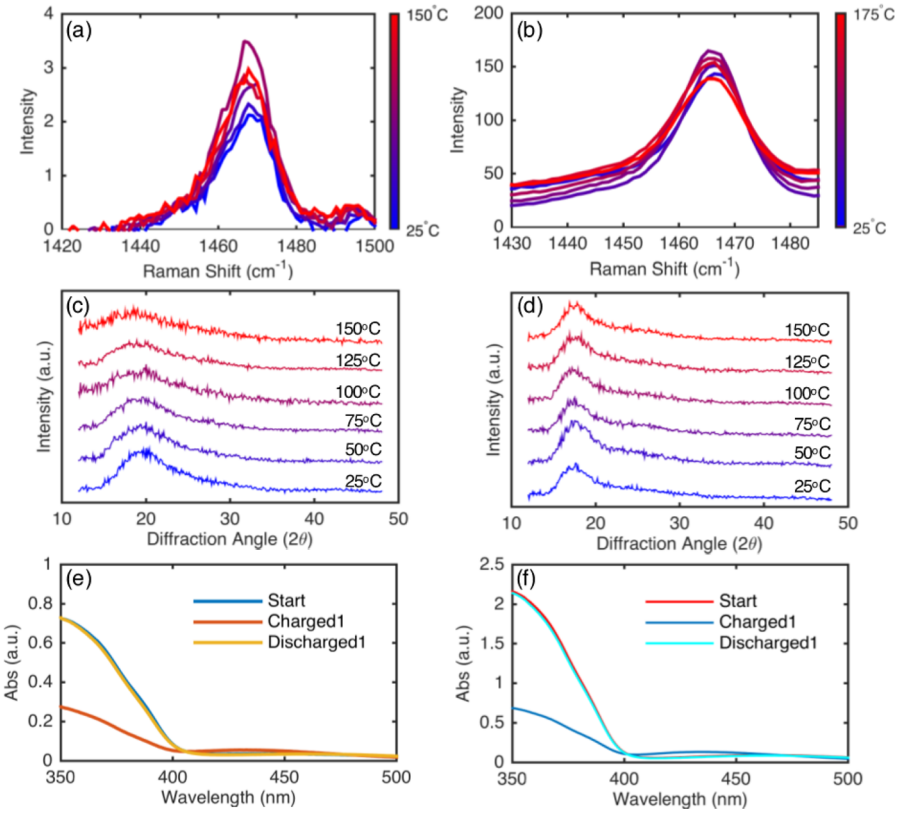

Figure 5. (a) Temperature resolved Raman mapping of compound **2** in film. No shift in the Raman peak and sharpness indicates that the state of the film is preserved throughout the heating process. (b) Temperature resolved Raman mapping of the compound **3** film. (c) Ex situ temperature XRD on the compound **2** film (scan time 60 s). (d) Ex situ temperature XRD on the compound **3** film (scan time 60 s). UV−vis spectrum of light charging and heat discharging of (e) compound **2** and (f) compound **3** films.

Bulkier Functionalization on Azobenzene Scaffold. Compound **1** was modified further by adding nonplanarity to the molecule, which has been suggested previously as a means to maintain the amorphous state at higher temperatures.[29] Molecules henceforth called compound **2** and compound **3** (Figure 1b) were synthesized to understand the effect of nonplanarity on the thermal stability, charging rate, and switchabilty of the molecule in the solid state. Compound **2** extends the existing planarity break with an additional phenyl group, while compound **3** breaks the planarity further and reduces stacking of the azobenzene derivatives due to $\pi-\pi$ interactions with the addition of a *tert*-butyl group. When the two compounds were spin-coated to a thin film, SEM showed that compound **2** and **3** had improved film morphology compared to that of compound **1** (Figures 4a and b). Compounds **2** and **3** resulted in films smoother and less grainy than those of compound **1**, indicating better propensity to make uniform and well-controlled thin films.

One important aspect of solid-state STF is the chargeability of the STF molecule in the solid-state. The chargeability of the solid-state films of compounds **1**, **2**, and **3** was characterized using ex situ photocharging and solid-state UV−vis spectroscopy. Figure 4c shows the *cis* fraction of the solid-state STF films based on photocharging time. The samples were prepared to give similar optical densities. The three compounds in the solid-state showed nearly identical $\pi \rightarrow \pi^*$ transitions centered at around 350 nm. The change in the UV−vis spectrum of each of the compounds with exposure time can be seen in the Supporting Information, section S3.

It is important to note two key properties that have improved from compound **1**. One is the charging rate, and the second is the photostationary state or the charged amount. First, to determine the charging rate at which the film changes from *trans* to *cis*, the first 140 s was linearly fitted from the time vs fraction of the *cis* graph (Supporting Information, Figure S3d). Compounds **2** and **3** showed over 65% increase in charging rate from that of compound **1**. Further, the addition of the bulky groups improved the photostationary state of the solid-state films. Compounds **1**, **2**, and **3** showed *cis* fractions of 0.60, 0.74, and 0.80, respectively, indicating that compounds **2** and **3** allow more complete charging of the solar thermal fuel. The bulky structures functionalized for compounds **2** and **3** act as spacers, which create additional free volume in the amorphous matrix and allow the molecules to undergo photoisomerization from *trans* to *cis* at a faster rate.

Figure 4d shows our DSC measurements for charged compounds **2** and **3**. Unlike compound **1**, both showed heat release in a single region with compound **2** (3 measurements), giving 100 ± 4 J/g or 88 ± 4 kJ/mol and compound **3** (3 measurements) giving 108 ± 2 J/g or 87 ± 2 kJ/mol. In both cases, the energy per molecule increased compared to that of compound **1**. The majority of the heat was released in the range of 75−125 °C for compound **2** and 90−175 °C for compound **3**. We note that the heat release trace is not a smooth peak and propose to attribute this to differences in activations energies for different subpopulations of molecules due to differences in local environment. Though the films are amorphous in either *cis* or *trans* state, slight spatial differences may arise due to a presence of a small fraction of *trans* isomer, as was seen with

DOI: 10.1021/acsami.6b15018
ACS Appl. Mater. Interfaces XXXX, XXX, XXX−XXX

compound **1** that had 2 release peaks. In certain applications, the ideal case would be for the heat release to proceed simultaneously; however, this also presents a potential avenue to control the rate of heat release once the precise intermolecular mechanisms for controlling the activation energy are better understood.

Importantly, both thin films of the synthesized materials showed thermal stability within these ranges of heat release. As can be seen in the optical images, the compound **2** film started dewetting at 150 °C, while the compound **3** film remained intact up to 175 °C (Supporting Information, Figures S2a and b). Temperature resolved Raman spectroscopy on the N═N azo bond stretch showed that in both cases the peak remained in the same position, indicating that compound **2** and **3** films remained in their amorphous states (Figure 5a and b). Ex situ temperature-dependent XRD showed that in both cases the film showed amorphous peaks and maintained its amorphous state throughout heating of the film (Figures 5c and d). The higher thermal stability of the compound **3** films confirmed that the addition of *tert*-butyl groups effectively prevents the $\pi-\pi$ stacking of the azobenzene derivative under thermal annealing conditions at higher temperatures. The switching of the solid-state film between the *trans* and *cis* states was confirmed using UV−vis spectroscopy (Figures 5e and f). The two films were charged using 365 nm UV light confirmed by the decrease in the $\pi \rightarrow \pi^*$ transition. However, this time, the discharge of the material was performed using thermal triggering. After charging, the film was placed in the dark at 100 °C for 2 h. Unlike the compound **1** film, the two films recovered the $\pi \rightarrow \pi^*$ transition peak fully with no observed morphological change and were able to charge once more. Additional switching of this can be seen in the Supporting Information, Figures S4a and b. In effect, compounds **2** and **3** prevent the films from undergoing irreversible morphology changes, thus allowing them to cycle many times. In contrast, compound **1** crystallizes after **1** charging/discharging cycle, making it impossible to charge again.

Table 1 shows the summary of heat storage properties and chargeability of azobenzene-based solid-state solar thermal fuels. The O and X indicates whether or not solid state changeability and solid state thermal switching is possible. Although a decrease in gravimetric energy density is observed, the addition of the phenyl and *tert*-butyl groups proved to be an effective strategy in improving the energy stored per molecule, chargeability, and thermal stability of the molecule. The energy stored per molecule for compounds **2** and **3** increased by more than 12% compared to that of compound **1**. The rate of charging for compounds **2** and **3** increased by 60% compared to that of compound **1**, while photostationary state in the solid state improved up to 33%. Of the two compounds, the additional symmetry breaking of compound **3** using the *tert*-butyl group was the most effective in improving thermal stability of the film, which increased to up to 175 °C with no signs of crystallization. This showed the effectiveness of molecular engineering for solid-state solar thermal fuel.

Table 1. Comparison of Heat Storage Properties, Chargeability, and Switching in the Solid State

	energy density (J/g)	energy density (kJ/mol)	solid state chargeability	solid state thermal switching
azobenzene[6,9]	161	49	X	X
azopolymer[10]	104	28	O	O
norbornadiene derivative[42]	629	124	X	X
compound **1**	134	77	O	X
compound **2**	100	88	O	O
compound **3**	108	87	O	O

CONCLUSIONS

Here, we demonstrated an effective molecular design to achieve solid-state STF materials with high energy density and thermal stability without the need for polymerization or templates. Through the functionalization of azobenzene with bulky aromatic groups, a new class of STF molecules was developed that enables high-energy storage per molecule (nearly 90 kJ/mol), which translates to over 30% improvement in solid-state energy storage density compared to the previously reported azobenzene-functionalized polymer, while promoting excellent solid-state film formation. Through additional molecular design, the rate of charging increased by 60%, and chargeability of the material improved by 33%. Also, the thermal stability of the solid-state film improved from ∼75 to 180 °C. Our results found that breaking the planarity of the molecule plays a crucial role on solar thermal fuel properties and sheds light on future directions for structural engineering of molecules to allow thermally stable and switchable STF thin films. We were able to simultaneously engineer the small molecule films to have increased energy density while also exhibiting excellent charging and cycling properties. More broadly, the film formation design principles that enable the deposition of stable amorphous films through solution processing can be applied to other areas such as organic photovoltaics and organic light-emitting diodes. With increasing requirements for solid-state integration of small molecules for functional devices, molecular films present a tremendous avenue in terms of versatility, ease of processing, and cost reduction.

ASSOCIATED CONTENT

Supporting Information

The Supporting Information is available free of charge on the ACS Publications website at DOI: 10.1021/acsami.6b15018.

Detailed schematic of the synthesis of compounds **2** and compound **3**, optical image of compounds **2** and compound **3**, solid-state optical charging, and charging and discharging of compound **2** and compound **3** films (PDF)

AUTHOR INFORMATION

Corresponding Author

*E-mail: jcg@mit.edu.

ORCID

Eugene N. Cho: 0000-0002-7093-8761

Notes

The authors declare no competing financial interest.

ACKNOWLEDGMENTS

E.N.C. acknowledges Bavarian Motor Works (BMW) for materials and resources for this project. D.Z. acknowledges his Natural Sciences and Engineering Research Council of Canada Banting Fellowship. The authors thank C.S. for help in setting up the XRD experiment. The authors also thank CMSE (Grant DMR 14-19807). The authors thank Ms. Li Li at MIT DCIF

DOI: 10.1021/acsami.6b15018
ACS Appl. Mater. Interfaces XXXX, XXX, XXX−XXX

(Department of Chemistry Instrumentation Facility) for high-resolution mass spectroscopy.

REFERENCES

(1) Philippopoulos, C.; Economou, D.; Economou, C.; Marangozis, J. Norbornadiene-Quadricyclane System in the Photochemical Conversion and Storage of Solar Energy. *Ind. Eng. Chem. Prod. Res. Dev.* **1983**, *22* (4), 627−633.
(2) Kuisma, M. J.; Lundin, A. M.; Moth-Poulsen, K.; Hyldgaard, P.; Erhart, P. Comparative Ab-Initio Study of Substituted Norbornadiene-Quadricyclane Compounds for Solar Thermal Storage. *J. Phys. Chem. C* **2016**, *120* (7), 3635−3645.
(3) Gray, V.; Lennartson, A.; Ratanalert, P.; Börjesson, K.; Moth-Poulsen, K. Diaryl-Substituted Norbornadienes with Red-Shifted Absorption for Molecular Solar Thermal Energy Storage. *Chem. Commun.* **2014**, *50* (40), 5330−5332.
(4) Kanai, Y.; Srinivasan, V.; Meier, S. K.; Vollhardt, K. P. C.; Grossman, J. C. Mechanism of Thermal Reversal of the (Fulvalene)-tetracarbonyldiruthenium Photoisomerization: Toward Molecular Solar−Thermal Energy Storage. *Angew. Chem., Int. Ed.* **2010**, *49* (47), 8926−8929.
(5) Boese, R.; Cammack, J. K.; Matzger, A. J.; Pflug, K.; Tolman, W. B.; Vollhardt, K. P. C.; Weidman, T. W. Photochemistry of (Fulvalene)tetracarbonyldiruthenium and Its Derivatives: Efficient Light Energy Storage Devices. *J. Am. Chem. Soc.* **1997**, *119* (29), 6757−6773.
(6) Olmsted, J., III; Lawrence, J.; Yee, G. G. Photochemical Storage Potential of Azobenzenes. *Sol. Energy* **1983**, *30* (3), 271−274.
(7) Kolpak, A. M.; Grossman, J. C. Azobenzene-Functionalized Carbon Nanotubes As High-Energy Density Solar Thermal Fuels. *Nano Lett.* **2011**, *11* (8), 3156−3162.
(8) Kolpak, A. M.; Grossman, J. C. Hybrid Chromophore/Template Nanostructures: A Customizable Platform Material for Solar Energy Storage and Conversion. *J. Chem. Phys.* **2013**, *138* (3), 034303.
(9) Kucharski, T. J.; Ferralis, N.; Kolpak, A. M.; Zheng, J. O.; Nocera, D. G.; Grossman, J. C. Templated Assembly of Photoswitches Significantly Increases the Energy-Storage Capacity of Solar Thermal Fuels. *Nat. Chem.* **2014**, *6* (5), 441−447.
(10) Zhitomirsky, D.; Cho, E.; Grossman, J. C. Solid-State Solar Thermal Fuels for Heat Release Applications. *Adv. Energy Mater.* **2016**, *6*, 1502006.
(11) Zhitomirsky, D.; Grossman, J. C. Conformal Electroplating of Azobenzene-Based Solar Thermal Fuels onto Large-Area and Fiber Geometries. *ACS Appl. Mater. Interfaces* **2016**, *8* (39), 26319−26325.
(12) Han, G. D.; Park, S. S.; Liu, Y.; Zhitomirsky, D.; Cho, E.; Dincă, M.; Grossman, J. C. Photon Energy Storage Materials with High Energy Densities Based on Diacetylene−azobenzene Derivatives. *J. Mater. Chem. A* **2016**, *4* (41), 16157−16165.
(13) Zhitomirsky, D.; Grossman, J. C. Conformal Electroplating of Azobenzene-Based Solar Thermal Fuels onto Large Area and Fiber Geometries. *ACS Appl. Mater. Interfaces* **2016**, *8*, 26319.
(14) Bushuyev, O. S.; Tomberg, A.; Friščić, T.; Barrett, C. J. Shaping Crystals with Light: Crystal-to-Crystal Isomerization and Photomechanical Effect in Fluorinated Azobenzenes. *J. Am. Chem. Soc.* **2013**, *135* (34), 12556−12559.
(15) Hagen, S.; Leyssner, F.; Nandi, D.; Wolf, M.; Tegeder, P. Reversible Switching of Tetra-Tert-Butyl-Azobenzene on a Au(1 1 1) Surface Induced by Light and Thermal Activation. *Chem. Phys. Lett.* **2007**, *444* (1−3), 85−90.
(16) Evans, S. D.; Johnson, S. R.; Ringsdorf, H.; Williams, L. M.; Wolf, H. Photoswitching of Azobenzene Derivatives Formed on Planar and Colloidal Gold Surfaces. *Langmuir* **1998**, *14* (22), 6436−6440.
(17) Bian, S.; Williams, J. M.; Kim, D. Y.; Li, L.; Balasubramanian, S.; Kumar, J.; Tripathy, S. Photoinduced Surface Deformations on Azobenzene Polymer Films. *J. Appl. Phys.* **1999**, *86* (8), 4498−4508.
(18) Kim, M.-J.; Shin, B.-G.; Kim, J.-J.; Kim, D.-Y. Photoinduced Supramolecular Chirality in Amorphous Azobenzene Polymer Films. *J. Am. Chem. Soc.* **2002**, *124* (14), 3504−3505.
(19) Jiang, X. L.; Li, L.; Kumar, J.; Kim, D. Y.; Shivshankar, V.; Tripathy, S. K. Polarization Dependent Recordings of Surface Relief Gratings on Azobenzene Containing Polymer Films. *Appl. Phys. Lett.* **1996**, *68* (19), 2618−2620.
(20) Enomoto, T.; Hagiwara, H.; Tryk, D. A.; Liu, Z.-F.; Hashimoto, K.; Fujishima, A. Electrostatically Induced Isomerization of Azobenzene Derivatives in Langmuir−Blodgett Films. *J. Phys. Chem. B* **1997**, *101* (38), 7422−7427.
(21) Shimomura, M.; Kunitake, T. Preparation of Langmuir-Blodgett Films of Azobenzene Amphiphiles as Polyion Complexes. *Thin Solid Films* **1985**, *132* (1−4), 243−248.
(22) Matsumoto, M.; Terrettaz, S.; Tachibana, H. Photo-Induced Structural Changes of Azobenzene Langmuir−Blodgett Films. *Adv. Colloid Interface Sci.* **2000**, *87* (2−3), 147−164.
(23) Cheng, L.; Torres, Y.; Lee, K. M.; McClung, A. J.; Baur, J.; White, T. J.; Oates, W. S. Photomechanical Bending Mechanics of Polydomain Azobenzene Liquid Crystal Polymer Network Films. *J. Appl. Phys.* **2012**, *112* (1), 013513.
(24) Fujii, T.; Kuwahara, S.; Katayama, K.; Takado, K.; Ube, T.; Ikeda, T. Molecular Dynamics in Azobenzene Liquid Crystal Polymer Films Measured by Time-Resolved Techniques. *Phys. Chem. Chem. Phys.* **2014**, *16* (22), 10485−10490.
(25) Ikeda, T. Photomodulation of Liquid Crystal Orientations for Photonic Applications. *J. Mater. Chem.* **2003**, *13* (9), 2037−2057.
(26) Taoda, H.; Hayakawa, K.; Kawase, K.; Yamakita, H. Photochemical Conversion and Storage of Solar Energy by Azobenzene. *J. Chem. Eng. Jpn.* **1987**, *20* (3), 265−270.
(27) Liu, Y.; Grossman, J. C. Accelerating the Design of Solar Thermal Fuel Materials through High Throughput Simulations. *Nano Lett.* **2014**, *14* (12), 7046−7050.
(28) Imahori, T.; Yamaguchi, R.; Kurihara, S. Azobenzene-Tethered Bis(Trityl Alcohol) as a Photoswitchable Cooperative Acid Catalyst for Morita−Baylis−Hillman Reactions. *Chem. - Eur. J.* **2012**, *18* (35), 10802−10807.
(29) Zhao, X.; Wang, S.; You, J.; Zhang, Y.; Li, X. Solution-Processed Thermally Stable Amorphous Films of Small Molecular Hole Injection/Transport Bi-Functional Materials and Their Application in High Efficiency OLEDs. *J. Mater. Chem. C* **2015**, *3* (43), 11377−11384.
(30) Baldo, M. A.; Soos, Z. G.; Forrest, S. R. Local Order in Amorphous Organic Molecular Thin Films. *Chem. Phys. Lett.* **2001**, *347* (4−6), 297−303.
(31) Naito, T.; Horie, K.; Mita, I. Photochemistry in Polymer Solids. 11. The Effects of the Size of Reaction Groups and the Mode of Photoisomerization on Photochromic Reactions in Polycarbonate Film. *Macromolecules* **1991**, *24* (10), 2907−2911.
(32) Feng, Y.; Liu, H.; Luo, W.; Liu, E.; Zhao, N.; Yoshino, K.; Feng, W. Covalent Functionalization of Graphene by Azobenzene with Molecular Hydrogen Bonds for Long-Term Solar Thermal Storage. *Sci. Rep.* **2013**, *3*, 1 DOI: 10.1038/srep03260.
(33) Luo, W.; Feng, Y.; Cao, C.; Li, M.; Liu, E.; Li, S.; Qin, C.; Hu, W.; Feng, W. A High Energy Density Azobenzene/Graphene Hybrid: A Nano-Templated Platform for Solar Thermal Storage. *J. Mater. Chem. A* **2015**, *3* (22), 11787−11795.
(34) Barrett, C.; Natansohn, A.; Rochon, P. Thermal Cis-Trans Isomerization Rates of Azobenzenes Bound in the Side Chain of Some Copolymers and Blends. *Macromolecules* **1994**, *27* (17), 4781−4786.
(35) Barrett, C.; Natansohn, A.; Rochon, P. Cis-Trans Thermal Isomerization Rates of Bound and Doped Azobenzenes in a Series of Polymers. *Chem. Mater.* **1995**, *7* (5), 899−903.
(36) Han, M.; Hara, M. Intense Fluorescence from Light-Driven Self-Assembled Aggregates of Nonionic Azobenzene Derivative. *J. Am. Chem. Soc.* **2005**, *127* (31), 10951−10955.
(37) Han, M.; Ishikawa, D.; Muto, E.; Hara, M. Isomerization and Fluorescence Characteristics of Sterically Hindered Azobenzene Derivatives. *J. Lumin.* **2009**, *129* (10), 1163−1168.
(38) Biswas, N.; Umapathy, S. Structures, Vibrational Frequencies, and Normal Modes of Substituted Azo Dyes: Infrared, Raman, and

DOI: 10.1021/acsami.6b15018
ACS Appl. Mater. Interfaces XXXX, XXX, XXX−XXX

Density Functional Calculations. *J. Phys. Chem. A* **2000**, *104* (12), 2734−2745.
(39) Stuart, C. M.; Frontiera, R. R.; Mathies, R. A. Excited-State Structure and Dynamics of Cis- and Trans-Azobenzene from Resonance Raman Intensity Analysis. *J. Phys. Chem. A* **2007**, *111* (48), 12072−12080.
(40) Yang, S. I.; Kim, K.-H.; Kang, D.; Joo, S.-W. Cis-to-Trans Photoconversion of Azobenzene Self-Assembled Monolayers on Gold Nanoparticle Surfaces Investigated by Raman Spectroscopy. *Photochem. Photobiol. Sci.* **2009**, *8* (1), 31−33.
(41) Armstrong, D. R.; Clarkson, J.; Smith, W. E. Vibrational Analysis of Trans-Azobenzene. *J. Phys. Chem.* **1995**, *99* (51), 17825−17831.
(42) Quant, M.; Lennartson, A.; Dreos, A.; Kuisma, M.; Erhart, P.; Börjesson, K.; Moth-Poulsen, K. Low Molecular Weight Norbornadiene Derivatives for Molecular Solar-Thermal Energy Storage. *Chem. - Eur. J.* **2016**, *22* (37), 13265−13274.

DOI: 10.1021/acsami.6b15018
ACS Appl. Mater. Interfaces XXXX, XXX, XXX−XXX